The Transport Properties of Carbon Dioxide

JOHN T. KENNEDY and GEORGE THODOS

The Technological Institute, Northwestern University, Evanston, Illinois

Experimental viscosity, thermal conductivity, and self-diffusivity data available in the literature for carbon dioxide have been critically reviewed and used to develop reduced state correlations of the transport properties for this substance. These correlations should apply to nonpolar compounds having critical compressibility factors approximately equal to that of carbon dioxide, $z_c = 0.275$.

In order to establish the dependence of these transport properties in the high pressure and liquid state regions, use has been made of relationships between the residual properties, μ-μ^*, k-k*, and $(P\mathcal{D})^*$-$(P\mathcal{D})$ and density. These residual quantities represent the differences between the values of the properties at any pressure and temperature and those at atmospheric pressure and the same temperature. These relationships also allow the determination of the values of the transport properties at the critical point. The resulting critical values along with the residual relationships enabled the construction of reduced state correlations for viscosity, thermal conductivity, and the product of self-diffusivity and pressure for carbon dioxide.

These correlations extend from the saturated vapor and liquid states to reduced temperatures of $T_R = 10$ and reduced pressures of $P_R = 50$. Comparisons made between values resulting from these correlations and corresponding experimental values, including the region of high pressure for both the gaseous and liquid states and the vicinity of the critical point, produced an average deviation of 2.0% for viscosity, 1.4% for thermal conductivity, and 5.9% for self-diffusivity.

Current interest in the field of nonequilibrium processes requires that values of the transport properties of fluids be available not only at moderate conditions but also at extremes of temperature and pressure. The viscosity, thermal conductivity, and self-diffusivity, μ, k, and $\mathcal{D}$ are defined by the basic relationships for momentum, heat, and mass transfer as follows:

$$\tau = -\mu \frac{du}{dx} \tag{1}$$

$$q = -k \frac{dt}{dx} \tag{2}$$

$$r = -\mathcal{D} \frac{dc}{dx} \tag{3}$$

Theoretical expressions defining the transport properties of gases in terms of intermolecular forces and collision integrals have been developed by Chapman and Cowling (*6*) and others. For the Lennard-Jones potential the collision integrals $\Omega^{(1,1)*}[T_N]$ and $\Omega^{(2,2)*}[T_N]$ have been evaluated by Hirschfelder, Bird, and Spotz (*13*) and can be used to determine the first approximation of viscosity, thermal conductivity, and self-diffusivity from the following relationships:

$$[\mu]_1 = 266.93 \times 10^{-5} \frac{\sqrt{MT}}{\sigma^2 \Omega^{(2,2)*}[T_N]} \tag{4}$$

$$[k]_1 = 19.891 \times 10^{-5} \frac{\sqrt{T/M}}{\sigma^2 \Omega^{(2,2)*}[T_N]} \tag{5}$$

$$[\mathcal{D}]_1 = 262.80 \times 10^{-5} \frac{\sqrt{T^3/M}}{P\sigma^2 \Omega^{(1,1)*}[T_N]} \tag{6}$$

The Lennard-Jones force constant ϵ/κ is used to define the normalized temperature $T_N = T/\frac{\epsilon}{\kappa}$ which in turn produced the collision integrals $\Omega^{(1,1)*}[T_N]$ and $\Omega^{(2,2)*}[T_N]$ from tabulated values (*14*). In order to obtain higher approximations of these transport properties the values resulting from Equations (4), (5), and (6) must be multiplied by the factors $f_\mu^{(3)}$, $f_k^{(3)}$, and $f_D^{(2)}$ presented elsewhere (*14*). These factors are essentially equal to unity over an extreme range of temperatures and never deviate by more than 1%.

Equations (4), (5), and (6) are rigorous for monatomic gases. For these gases Shimotake and Thodos (*48*) found that good agreement exists between experimental viscosity values and the results obtained with Equation (4). For thermal conductivity Owens and Thodos (*37*) found that values calculated with Equation (5) were consistent with experimental measurements for the monatomic gases. For polyatomic gases the Eucken correction factor (*9*) must be applied to Equation (5) to account for the rotational and vibrational energy contributions. Viscosities and thermal conductivities calculated with Equations (4) and (5) have been found to be pressure insensitive from 5 mm. of mercury (*4, 45*) up to 10 atm. On the other hand Equation (6) indicates that the self-diffusivity is inversely proportional to pressure for these moderate pressure conditions. In order to eliminate the effect of pressure Equation (6) can be rearranged to yield the product $P\mathcal{D}$. Thus the viscosity, the thermal conductivity, and the product of pressure and self-diffusivity become unique functions of the same variables.

Reliable critical values are necessary for the treatment of transport properties. For carbon dioxide the critical values presented by Michels, Blaisse, and Michels (*31*) $T_c = 304.2$°K., $P_c = 72.85$ atm., and $\rho_c = 0.467$g./cc. have been used to produce the critical volume and critical compressibility factor $v_c = 94.24$ cc./g.-mole and $z_c = 0.275$.

TRANSPORT PROPERTIES AT MODERATE PRESSURES

Experimental data for the three transport properties have been obtained from literature sources and utilized to determine their dependence upon both temperature and pressure. For viscosity and thermal conductivity the effect of pressure is negligible for pressures between 2.5 and 760 mm. of mercury, and therefore the variation of these properties in this pressure interval is a function of temperature only. However self-diffusivity is a function of both temperature and pressure.

Viscosity

Experimental viscosity data for pressures ranging from 2.5 to 760 mm. of mercury are presented in Figure 1. The viscosity data of eight investigators are presented in Figure 1 and appear to be internally consistent. In addition the data of eight other investigators (*8, 15, 28, 49, 53, 59, 61, 64*) covering the same range were examined and were found to agree with the data presented in Figure 1.

The variation of viscosity for moderate pressures has been related for $T_R = 0.65$ to $T_R = 5.5$. This relationship enables the determination of viscosity at moderate pressure and the critical temperature $\mu^*_{T_c} = 1{,}520 \times 10^{-5}$ centipoises.

The viscosity data considered most reliable have been utilized to calculate the Lennard-Jones force constants σ and ϵ/κ. The values resulting from pairs of viscosity values are presented in Table 1 and when averaged produced $\sigma = 3.876$Å. and $\epsilon/\kappa = 216$°K. Hirschfelder, Curtiss, and Bird (*14*) present two sets for the Lennard-Jones force constants of carbon dioxide: $\sigma = 3.976$Å., $\epsilon/\kappa = 190$°K. and $\sigma = 3.897$Å., $\epsilon/\kappa = 213$°K. The Lennard-Jones force constants produced from the present study have been used with Equation (4) to calculate viscosities for temperatures ranging from $T_R = 0.4$ to $T_R = 10$ which were found

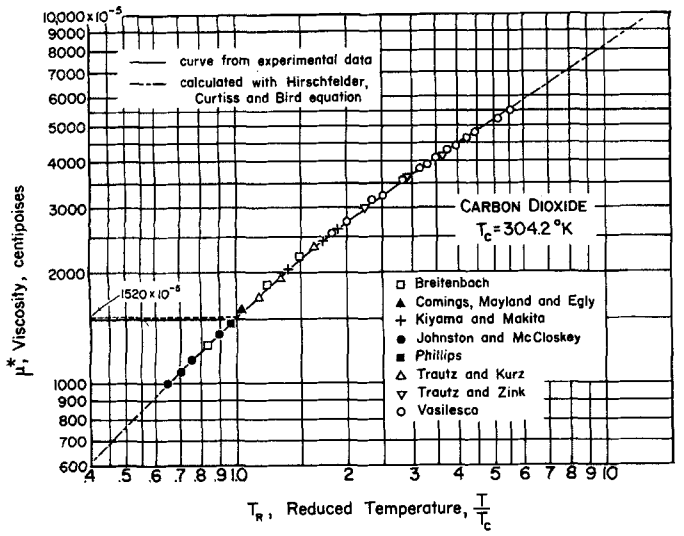

Fig. 1. Variation of viscosity with temperature at atmospheric pressure for carbon dioxide.

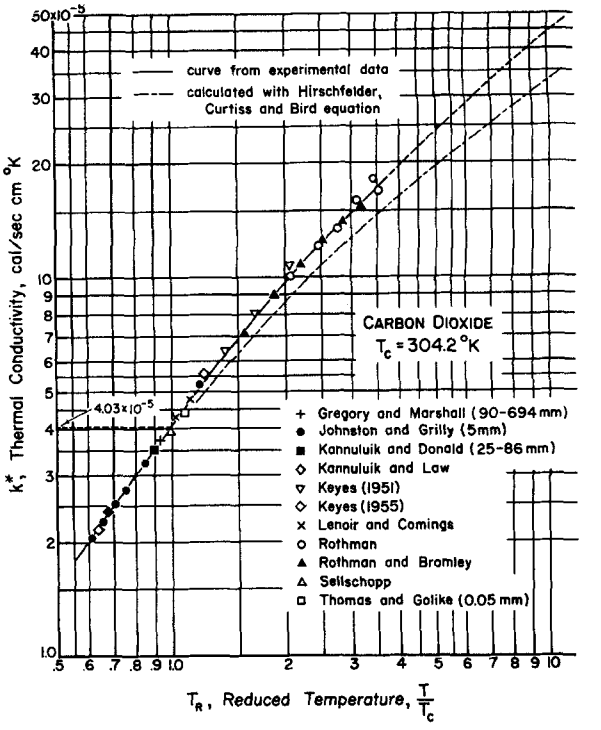

Fig. 2. Variation of thermal conductivity with temperature for carbon dioxide at pressures of 1 atm. and lower.

to coincide with the experimental values presented in Figure 1.

Thermal Conductivity

A review of the experimental thermal conductivity values for carbon dioxide reported by a number of investigators has been made over the pressure range 0.05 to 760 mm. of mercury. The thermal conductivity was found to be insensitive in this pressure range. Experimental points are plotted in Figure 2 and cover the temperature range of $T_R = 0.6$ to $T_R = 3.5$.

This correlation shows that the data of Thomas and Golike (52) obtained at a pressure of 0.05 mm. of mercury and also those of Johnston and Grilly (17) at 5 mm. of mercury coincide with the data obtained at atmospheric pressure. From Figure 2 the thermal conductivity at moderate pressures and the critical temperature is found to be $k^*_{T_c} = 4.03 \times 10^{-5}$ cal./sec. cm. °K.

Thermal conductivities have been calculated with Equation (5) corrected with the Eucken factor (9), (4/15) $C_v/R + 3/5$. For this factor, heat capacity data were obtained from two references (12, 41). A comparison of the calculated values and the experimental data is shown in Figure 2. Although these curves are similar, the calculated values at the higher temperatures are lower than the corresponding experimental values. Studies with the monatomic gases (37) indicate good agreement between experimental values and values calculated with Equation (5). Therefore this equation is valid for monatomic gases and does not require the use of the Eucken correction factor. The observed discrepancy between the experimental and calculated values for carbon dioxide is probably not caused by incorrect heat capacity values but most likely can be attributed to the Eucken correction factor which apparently is inexact for polyatomic gases.

In order to extend the experimental data above $T_R = 3.5$ calculated thermal conductivity values were plotted against experimental values on log-log coordinates for the same temperatures. The resulting straight line was extrapolated to cover the higher temperature region and thus enabled the extension of the experimental curve indicated with dashed lines.

Self-Diffusivity

Because of the limited number of experimental self-diffusivities available at atmospheric pressure the variation of this transport property cannot be properly defined over the range of temperature covered by the comparable treatments for viscosity and thermal conductivity. In order to obtain the basic atmospheric isobar Equation (6) has been applied to the calculation of self-diffusivities in the temperature interval of $T_R = 0.3$ and $T_R = 10$.

The values calculated with Equation (6) have been used to define the dashed portion of the curve of Figure 3. In addition the experimental atmospheric pressure data of Winn (63) and Timmerhaus and Drickamer (55) are also presented and are found to agree with the values produced by Equation (6).

EFFECT OF PRESSURE ON TRANSPORT PROPERTIES

For the thermal conductivity of gases at high pressures and of liquids the effect of pressure and temperature can be eliminated by the method of Abas-zade (1). This is accomplished through the introduction of the residual thermal conductivity k-k^* which is related directly to the density at the temperature and pressure of the system. The quantity k-k^* represents the increase in thermal conductivity due to the increase in pressure above 1 atm. at constant temperature. The thermal conductivity studies on the monatomic and diatomic gases (37, 45) show that a single continuous function for the gaseous and liquid states results when k-k^* is plotted against density on log-log coordinates.

For the monatomic and diatomic gases (4, 48) this approach has been applied to viscosities where the residual viscosity μ-μ^* is related to the density of the fluid. In order to apply this residual approach to carbon dioxide it is necessary to obtain first-density values for the corresponding temperatures and pressures of interest. The density data of several investigators (2, 16, 21, 22, 31, 33, 34, 39) were used to produce a reduced density correlation for carbon dioxide for both the gaseous and liquid states (22).

The available experimental viscosity data for carbon dioxide at high pressures in both the gaseous and liquid states and the atmospheric viscosities obtained from Figure 1 permit the calculation of residual viscosities μ-μ^*. When these values were related to their respective reduced densities ρ_R,

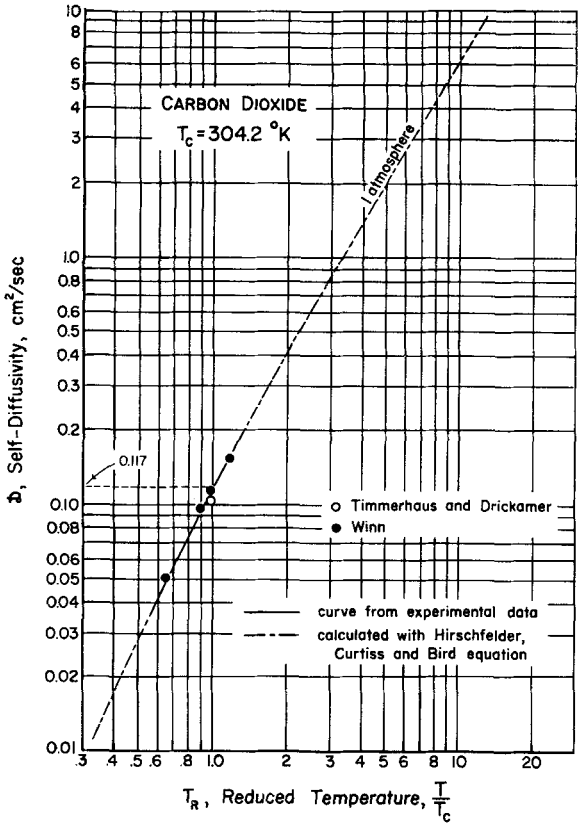

Fig. 3. Variation of self-diffusivity with temperature at 1 atm. for carbon dioxide.

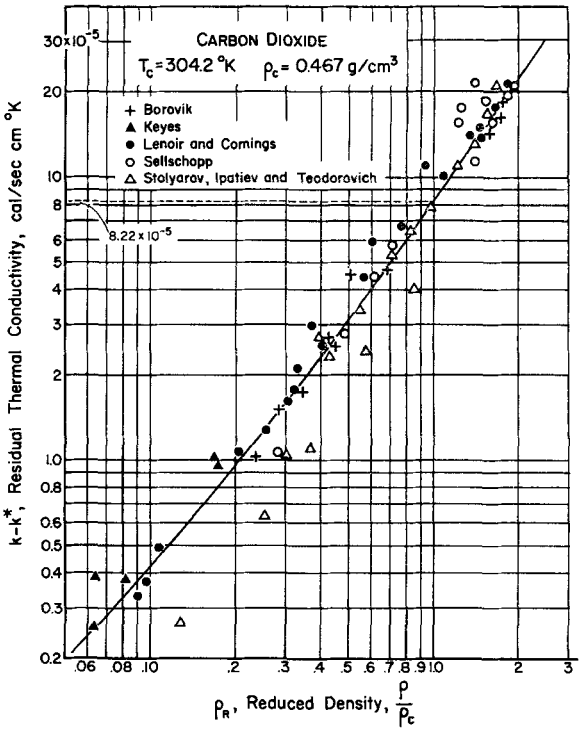

Fig. 5. Relationship of residual thermal conductivity and reduced density of carbon dioxide in the gaseous and liquid states.

the correlation presented in Figure 4 was produced. The recent experimental data in the vicinity of the critical point reported by Michels, Botzen, and Schuurman (32) are in excellent agreement with the liquid data of Stakelbeck (50) and those of Phillips (38) and Comings, Mayland, and Egly (7). The resulting relationship is continuous for the gaseous and liquid states of carbon dioxide. This relationship enables the estimation of the residual viscosity at the critical point $(\mu-\mu^*)_c = 1{,}815 \times 10^{-5}$ centipoises. When one uses this value and the viscosity of carbon dioxide at atmospheric pressure and $T_R = 1.0$ obtained from Figure 1, $\mu^* T_c = 1{,}520 \times 10^{-5}$ centipoises, the viscosity at the critical point μ_c is calculated to be 3335×10^{-5} centipoises. The ratio of these viscosities produces a value of 2.194 as the constant for the relationship

$$\mu_c = 2.194\, \mu^* T_c \qquad (7)$$

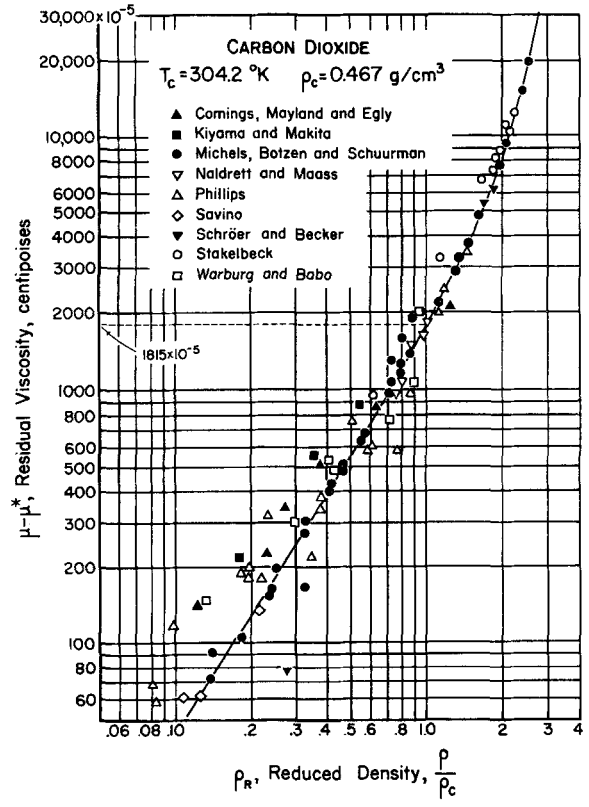

Fig. 4. Relationship of residual viscosity and reduced density for carbon dioxide in the gaseous and liquid states.

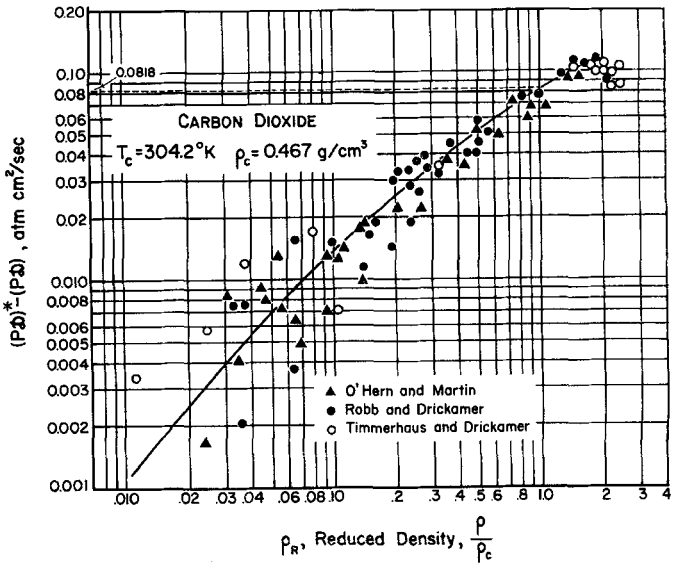

Fig. 6. Relationship of residual product of pressure and self-diffusivity with reduced density for carbon dioxide in the gaseous and dense phase regions.

TABLE 1. LENNARD-JONES FORCE CONSTANTS CALCULATED FROM VISCOSITY DATA

	T, °K.	$\mu \times 10^5$, centipoises	σ, Å.	ϵ/κ, °K.
Johnston and McCloskey (*18*)	198.0	1,005.9		
Kiyama and Makita (*27*)	423.2	2,050	3.900	209
Johnston and McCloskey (*18*)	286.6	1,431.2		
Kiyama and Makita (*27*)	423.2	2,050	3.821	233
Trautz and Kurz (*56*)	500.1	2,354		
Trautz and Zink (*57*)	672.2	2,982	3.864	220
Vasilesco (*60*)	759.4	3,260		
Vasilesco (*60*)	1,281.2	4,655	3.917	203
			3.876	216

A similar analysis was applied to the thermal conductivity data of carbon dioxide at high pressures in both the gaseous and liquid states. The relationship between the residual thermal conductivities and reduced densities obtained from the data of several investigators was found to be internally consistent as shown in Figure 5. The residual thermal conductivity at the critical density is found to be $(k\text{-}k^*)_c = 8.22 \times 10^{-5}$ cal./sec. cm. °K. The corresponding value at atmospheric pressure and the critical temperature $k^*_{T_c} = 4.03 \times 10^{-5}$ cal./sec. cm. °K. permits the calculation of the critical thermal conductivity $k_c = 12.25 \times 10^{-5}$ cal./sec. cm. °K. The ratio of these thermal conductivities 3.040 produces the constant for the relationship

$$k_c = 3.040\, k^*_{T_c} \qquad (8)$$

Guildner (*11*) reports that the thermal conductivity of carbon dioxide shows a sharp rise near the critical point. However this study indicates that this property should be continuous in the critical region. This difference could be attributed to the fact that in experimental measurements near the critical point convective effects are unavoidably present. Since self-diffusivity is pressure sensitive, it becomes necessary to introduce a residual quantity involving both the pressure and the self-diffusivity. An examination of Equation (6) suggests that the product of pressure and self-diffusivity $P\mathcal{D}$ should be dependent only upon temperature and the Lennard-Jones force constants. Through this reasoning it appears that the product $P\mathcal{D}$ should be applicable to a residual treatment as were viscosity and thermal conductivity. The application of this approach produced positive differences for the quantity $(P\mathcal{D})^* - (P\mathcal{D})$. These residual values were related to reduced density to produce the curve of Figure 6. The available high-pressure data for gaseous carbon dioxide of Timmerhaus and Drickamer (*54*), O'Hern and Martin (*36*), and Robb and Drickamer (*40*) were utilized in the development of this relationship. A review of their experimental values indicates some scattering, particularly in the lower density region. The fact that for this property the correlation is not as precise as that for viscosity and thermal conductivity should not reflect on the method, since reliable self-diffusivity data are not readily obtainable. It is important to point out that discrepancies of as much as 50% between reported values are not uncommon for the same temperature and pressure conditions.

Since no liquid self-diffusivity data are available, the correlation presented in Figure 6 has been restricted to the calculation of the product $P\mathcal{D}$ for the gaseous state only. Until such data can be obtained, the relationship of Figure 6 cannot be applied properly to the liquid state. Following an approach analogous to that used for viscosity and thermal conductivity, one can obtain the product $P\mathcal{D}$ at the critical point from the residual quantity at $\rho_R = 1.0$ as $(P\mathcal{D})^* - (P\mathcal{D}) = 0.0818$. From Figure 3 $(P\mathcal{D})^*_{T_c} = 0.117$, and there-

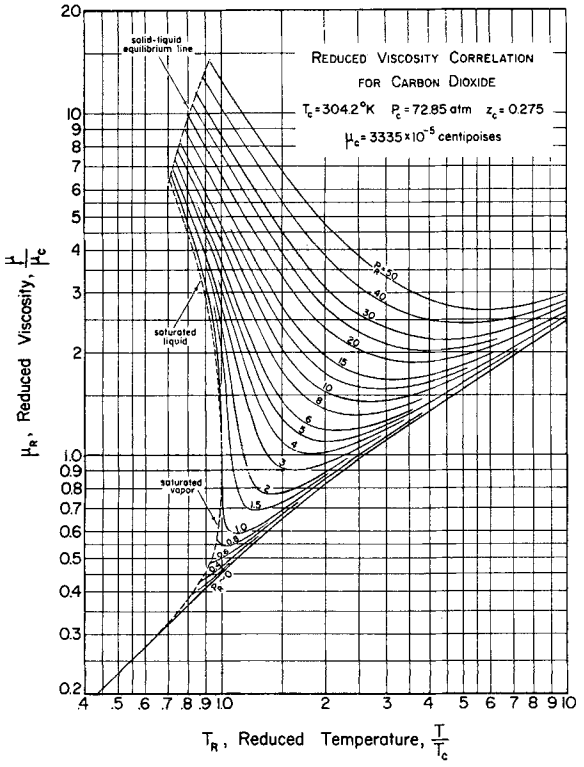

Fig. 7. Reduced viscosity correlation for carbon dioxide.

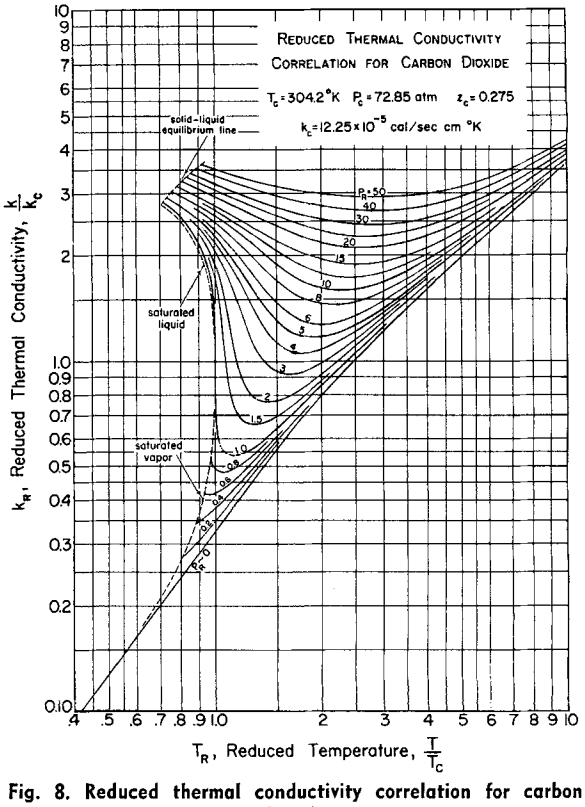

Fig. 8. Reduced thermal conductivity correlation for carbon dioxide.

fore at the critical point the product $(P\mathcal{D})_c = 0.0352$ atm. sq.cm./sec. The product $(P\mathcal{D})_c$ is equivalent to $P_c\mathcal{D}_c$ and thus enables the direct evaluation of the self-diffusivity of carbon dioxide at the critical point as $\mathcal{D}_c = 0.0352/72.85 = 48.32 \times 10^{-5}$ sq.cm./sec. The above values allow the calculation of the constant 0.3009 for the relationship

$$(P\mathcal{D})_c = 0.3009\,(P\mathcal{D})^*_{T_c} \qquad (9)$$

Information available in the literature for the transport properties of substances having critical compressibility factors similar to those of carbon dioxide should be analyzed to determine if Equations (7), (8), and (9) represent generalizations for this class of substances.

The residual relationships for viscosity, thermal conductivity, and the product $P\mathcal{D}$ are utilized in this study for the estimation of these transport properties in regions where data are lacking. Although the residual viscosity and thermal conductivity relationships presented in Figures 4 and 5 apply to both the gaseous and liquid states, it would be highly desirable to obtain self-diffusivities for liquid carbon dioxide so that Figure 6 will include properly the liquid state.

REDUCED STATE CORRELATIONS

The residual relationship for viscosity presented in Figure 4 along with the information of Figure 1 for viscosities at moderate pressures enables the calculation of viscosity at different temperatures and pressures for both the gaseous and liquid states. An enlarged plot of the reduced density of carbon dioxide for both the gaseous and liquid regions (23) was used in the calculation of viscosity values. Reduced densities corresponding to a specific temperature and pressure produced residual viscosities μ-μ^* from Figure 4. For these conditions a viscosity value for carbon dioxide could be readily obtained from the residual viscosity and the corresponding viscosity at moderate pressure μ^* obtained from Figure 1. These calculated viscosity values were then reduced with the critical value $\mu_c = 3{,}335 \times 10^{-5}$ centipoises to produce the reduced state correlation for carbon dioxide presented in Figure 7. This correlation is similar to the generalized viscosity correlation developed by Uyehara and Watson (58).

A similar approach has been utilized to establish the reduced thermal conductivity correlation presented in Figure 8. In its development the residual thermal conductivity plot of Figure 5 and the thermal conductivities at moderate pressures presented in Figure 2 have been utilized. This correlation is similar to the reduced state correlation of thermal conductivity for the monatomic gases (37).

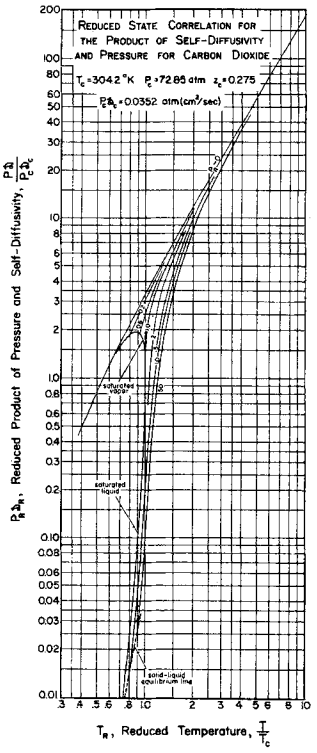

Fig. 9. Reduced state correlation for the product of self-diffusivity and pressure for carbon dioxide.

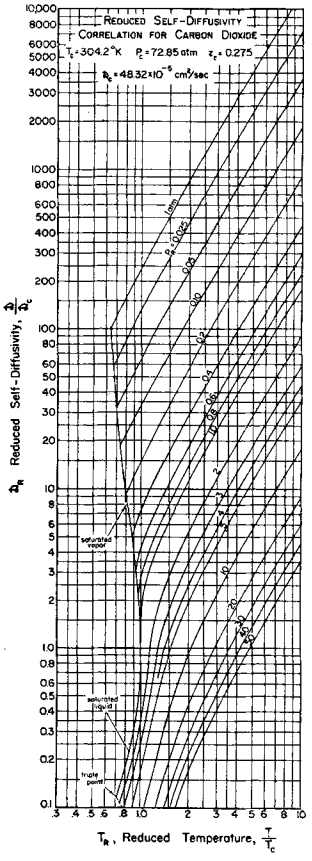

Fig. 10. Reduced self-diffusivity correlation for carbon dioxide.

The application of the residual correlation for $P\mathcal{D}$ to both the gaseous and liquid states is questionable because no liquid self-diffusivity values have been reported in the literature for carbon dioxide. In view of this limitation values of self-diffusivity for only the gaseous state have been calculated with the residual approach. With this restriction the product of $P\mathcal{D}$ has been calculated for several pressures and temperatures in the same manner as viscosity and thermal conductivity. These quantities can then be directly reduced with the critical value $(P\mathcal{D})_c = 0.0352$ atm. sq.cm./sec. to produce the dimensionless modulus $P_R\mathcal{D}_R$. The results of this development are presented in Figure 9. In order to extend this information into the liquid region self-diffusivity values were calculated from the modified form of the Stokes-Einstein equation proposed by Li and Chang (30):

$$\frac{\mathcal{D}\mu}{\kappa T} = \frac{1}{2\pi}\left(\frac{N}{v}\right)^{1/3} \qquad (10)$$

By using saturated liquid density values for carbon dioxide and the corresponding saturated viscosity values obtained from Figure 7 self-diffusivities were calculated at several temperatures with the following results:

T_R	P_R	$\mathcal{D}$, sq. cm./sec.	$P_R\mathcal{D}_R$
0.711	0.0565	5.636×10^{-5}	0.00659
0.75	0.0976	6.818	0.01378
0.80	0.1288	8.507	0.02268
0.85	0.2007	11.24	0.04668
0.90	0.3294	14.60	0.09953
0.95	0.5668	19.43	0.2279

These reduced products $P_R\mathcal{D}_R$ have been used to establish the saturated liquid line in Figure 9. In order to extend this information into the high pressure liquid region Equation (10) has been based on the saturated liquid line of the product of pressure and self-diffusivity $(P\mathcal{D})_s$, the saturated viscosity μ_s, and the saturated density ρ_s to produce the following relationship which accounts for the effect of pressure at isothermal conditions:

$$\frac{\mathcal{D}\mu}{\mathcal{D}_s\mu_s} = \left(\frac{v_s}{v}\right)^{1/3} \qquad (11)$$

With the use of the reduced density correlation (23) and the viscosity plot of Figure 7 Equation (11) allows the calculation of self-diffusivity values in the high-pressure region of the liquid state and thus permits the extension of the $P_R = 50$ isobar to the solid-liquid equilibrium line.

Figure 9 is similar to the reduced viscosity and thermal conductivity plots presented in Figures 7 and 8. The abrupt decrease of the product $P\mathcal{D}$ for the saturated liquid state deserves some explanation, since this

region has been approximated from the Li-Chang equation. It would prove interesting to check this region when experimental self-diffusivity values for liquid carbon dioxide become available.

With the elimination of pressure as a variable in the product $P\mathcal{D}$ it now becomes possible to construct a reduced state correlation involving only self-diffusivity. This has been accomplished by the use of the information available in Figure 9 to produce the reduced self-diffusivity correlation of Figure 10. In Figure 10 the self-diffusivity at moderate pressures does not approach a limiting value of $\mathcal{D}_R$ as was the case with viscosity and thermal conductivity. Instead the reduced self-diffusivity $\mathcal{D}_R$ continues to be directly related to pressure.

RELIABILITY OF TRANSPORT PROPERTY CORRELATIONS

The accuracy of the reduced state correlations for viscosity, thermal conductivity, and self-diffusivity presented in Figures 7, 8, and 10 has been tested with available literature data. Experimental values for gaseous and liquid carbon dioxide, when compared with values resulting from these reduced state correlations, produced the following average deviations:

	No. of experimental values (gas and liquid)	Average deviation
Viscosity	125	2.03%
Thermal conductivity	79	1.38
Self-diffusivity	91	13.6

If thirteen of the 91 experimental self-diffusivity values showing the highest deviations are excluded from this comparison, the average deviation is reduced to 5.93%.

These average values represent the deviations between values determined from the respective reduced state correlations and the corresponding experimental values. Since these experimental points have an undetermined degree of experimental error inherent in their determination, the values produced from these correlations could quite possibly be even closer to the actual values of the transport properties than the average deviations would indicate.

NOTATION

c = concentration, g.-moles/cc.
C_v = heat capacity at constant volume, cal./g.-mole °K.
$\mathcal{D}$ = self-diffusivity, sq.cm./sec.
$f_\mu^{(3)}$, $f_k^{(3)}$, $f_D^{(2)}$ = factors of higher approximations for viscosity, thermal conductivity, and self-diffusivity
k = thermal conductivity, cal./sec. cm. °K.
k^* = thermal conductivity at moderate pressures, cal./sec. cm. °K.
k_c = critical thermal conductivity, cal./sec. cm. °K.
k_R = reduced thermal conductivity, k/k_c
$k^*_{T_c}$ = thermal conductivity at moderate pressures and the critical temperature, cal./sec. cm. °K.
M = molecular weight
N = Avogadro number, 6.0238×10^{23} molecules/g.-mole
q = rate of heat transfer, cal./sec. sq. cm.
R = gas constant, 1.987 cal./g.-mole °K.
r = rate of mass transfer, g.-moles/sec. sq. cm.
t = temperature, °C.
T = absolute temperature, °K.
T_c = critical temperature, °K.
T_N = normalized temperature, $T/\frac{\epsilon}{\kappa}$
T_R = reduced temperature, T/T_c
u = velocity, cm./sec.
v = molar volume, cc./g.-mole
x = linear dimension, cm.

Greek Letters

ϵ = maximum energy of attraction for Lennard-Jones potential, erg.
κ = Boltzmann constant, 1.38047×10^{-16} erg./°K.
μ = viscosity, centipoises
μ^* = viscosity of gases at atmospheric pressure, centipoises
μ_c = viscosity at the critical point, centipoises
μ_R = reduced viscosity, μ/μ_c
$\mu^*_{T_c}$ = viscosity of gases at atmospheric pressure and critical temperature, centipoises
ρ = density, g./cc.
ρ_c = critical density, g./cc.
ρ_R = reduced density, ρ/ρ_c
σ = collision diameter for Lennard-Jones potential, Å.
τ = shear stress, dynes/sq. cm.
$\Omega^{(1,1)*}[T_N]$ = collision integral function for Lennard-Jones potential
$\Omega^{(2,2)*}[T_N]$ = collision integral function for Lennard-Jones potential

LITERATURE CITED

1. Abas-zade, A. K., *Zhur. Eksptl. i Teoret. Fiz.*, **23**, 60 (1952).
2. Amagat, E. H., *Compt. rend.*, **113**, 446 (1891).
3. Borovik, E., *Zhur. Eksptl. i Teoret. Fiz.*, **19**, 561 (1949).
4. Brebach, W. J., and George Thodos, *Ind. Eng. Chem.*, **50**, 1095 (1958).
5. Breitenbach, Paul, *Ann. Physik*, (4), **5**, 166 (1901).
6. Chapman, Sydney, and T. G. Cowling, "Mathematical Theory of Non-Uniform Gases," Cambridge University Press, Teddington, England (1939).
7. Comings, E. W., B. J. Mayland, and R. S. Egly, *Univ. Illinois Eng. Expt. Station Bull. 354* (1944).
8. Eglin, J. M., *Phys. Rev.*, **22**, 161 (1923).
9. Eucken, Arnold, *Z. Physik*, **14**, 324 (1913).
10. Gregory, Hamar, and Sybil Marshall, *Proc. Roy. Soc. (London)*, **114**, 354 (1927).
11. Guildner, L. A., *Proc. Natl. Acad. Sci.*, **44**, 1149 (1958).
12. Hilsenrath, Joseph, C. W. Beckett, W. S. Benedict, Lilla Fano, H. J. Hoge, J. F. Masi, R. L. Nuttall, Y. S. Touloukian, and H. W. Woolley, *Natl. Bur. Standards Circ. 564*, p. 163-4, U.S. Department of Commerce, Washington, D. C. (1955).
13. Hirschfelder, J. O., R. B. Bird, and E. L. Spotz, *J. Chem. Phys.*, **16**, 968-981 (1948).
14. Hirschfelder, J. O., C. F. Curtiss, and R. B. Bird, "Molecular Theory of Gases and Liquids," p. 1111-1130, Wiley, New York (1954).
15. Ishida, Yoshio, *Phys. Rev.*, **21**, 550 (1923).
16. Jenkins, C. F., and D. R. Pye, *Phil. Trans. Roy. Soc. (London)*, **A213**, 67 (1914).
17. Johnston, H. L., and E. R. Grilly, *J. Chem. Phys.*, **14**, 223 (1946).
18. Johnston, H. L., and K. E. McCloskey, *ibid.*, **44**, 1038 (1940).
19. Kannuluik, W. G., and H. B. Donald, *Australian J. Sci. Research*, **3A**, 417 (1950).
20. Kannuluik, W. G., and P. G. Law, *Proc. Roy. Soc. (Victoria)*, **58**, 142 (1947).
21. Keesom, W. H., *Communs. Phys. Lab. Univ. Leiden*, No. 88 (1903).
22. Kennedy, G. C., *Am. J. Sci.*, **252**, 225 (1954).
23. Kennedy, J. T., M.S. thesis, Northwestern University, Evanston, Illinois (1958).
24. Keyes, F. G., *Trans. Am. Soc. Mech. Engrs.*, **73**, 597 (1951).
25. *Ibid.*, **77**, 1395 (1955).
26. Kiyama, Ryo, and Tadashi Makita, *Rev. Phys. Chem. Japan*, **21**, 63 (1951).
27. *Ibid.*, **22**, 49 (1952).
28. Lasalle, L. J., *Phys. Rev.*, **17**, 354 (1921).
29. Lenoir, J. M., and E. W. Comings, *Chem. Eng. Progr.*, **47**, 223 (1951).
30. Li, J. C. M., and Pin Chang, *J. Chem. Phys.*, **23**, 518 (1955).
31. Michels, A., B. Blaisse, and C. Michels, *Proc. Roy. Soc. (London)*, **160**, 358 (1937).
32. Michels, A., A. Botzen, and W. Schuurman, *Physica*, **23**, 95 (1957).
33. Michels, A., and C. Michels, *Proc. Roy Soc. (London)*, **153**, 201 (1935).
34. ————, and H. Wouters, *ibid.*, p. 214.
35. Naldrett, S. N., and Otto Maass, *Can. J. Research*, **18B**, 322 (1940).
36. O'Hern, H. A., Jr., and J. J. Martin, *Ind. Eng. Chem.*, **47**, 2081 (1955).
37. Owens, E. J., and George Thodos, *A.I.Ch.E. Journal*, **3**, 454-61 (1957).

38. Phillips, P., *Proc. Roy. Soc. (London)*, **87**, 48 (1912).
39. Plank, R., and J. Kuprianoff, *Z. tech. Physik*, **10**, 93 (1929).
40. Robb, W. L., and H. G. Drickamer, *J. Chem. Phys.*, **19**, 1504 (1951).
41. Rossini, F. D., K. S. Pitzer, R. L. Arnett, R. M. Braun, and G. C. Pimental, *Am. Petroleum Inst. Proj. 44*, p. 631, Carnegie Press, Pittsburgh, Pennsylvania (1953).
42. Rothman, A. J., *U.S. Atomic Energy Comm. Tech. Inform. Service, UCRL 2339* (1954).
43. ———, and L. A. Bromley, *Ind. Eng. Chem.*, **47**, 899 (1955).
44. Savino, J. M., Ph.D. thesis, Purdue University, Lafayette, Indiana (1955).
45. Schaefer, C. A., and George Thodos, *A.I.Ch.E. Journal*, **5**, 367 (1959).
46. Schröer, Erich, and Gerhard Becker, *Z. physik. Chem.*, **A173**, 178 (1935).
47. Sellschopp, Wilhelm, *Forsch. Gebiete Ingenieurw.*, **5**, 162 (1934).
48. Shimotake, Hiroshi, and George Thodos, *A.I.Ch.E. Journal*, **4**, 257 (1958).
49. Smith, C. J., *Proc. Phys. Soc. (London)*, **34**, 155 (1922).
50. Stakelbeck, H., *Z. ges. Kälte-Ind.*, **40**, 33 (1933).
51. Stolyarov, E. A., V. V. Ipatiev, and P. Teodorovich, *Zhur. Fiz. Khim.*, **24**, 166 (1950).
52. Thomas, L. B., and R. C. Golike, *J. Chem. Phys.*, **22**, 300 (1954).
53. Thomson, Ernst, *Ann. Physik*, **36**, 815 (1911).
54. Timmerhaus, K. D., and H. G. Drickamer, *J. Chem. Phys.*, **20**, 981 (1952).
55. *Ibid.*, **19**, 1242 (1951).
56. Trautz, Max, and Friedrich Kurz, *Ann. Physik*, **9**, No. 5, p. 981 (1931).
57. Trautz, Max, and Robert Zink, *ibid.*, **10**, 427 (1930).
58. Uyehara, Otto, and K. M. Watson, *Natl. Petrol. News, Tech. Sect.*, **36**, R764 (October 4, 1944).
59. Van Dyke, K. S., *Phys. Rev.*, **21**, 250 (1923).
60. Vasilisco, Virgile, *Ann. Physik*, **20**, No. 6, p. 292 (1945).
61. Vogel, Hans, *ibid.*, **43**, No. 4, p. 1235 (1914).
62. Warburg, E. G., and Lambert Babo, *Ann. Physik Chem.*, **17**, 390 (1882).
63. Winn, E. B., *Phys. Rev.*, **80**, 1024 (1950).
64. Wüllner, F. H. A. A., *Ann. Physik*, **4**, 321 (1878).

Manuscript received February 18, 1960; revision received October 24, 1960; paper accepted October 26, 1960.

The Effect of Organic Substances on the Transfer of Oxygen from Air Bubbles in Water

W. WESLEY ECKENFELDER, JR., and EDWIN L. BARNHART

Manhattan College, New York, New York

The liquid film coefficient is related to bubble diameter and velocity in pure water and to the physical properties of the liquid. The addition to water of organic substances which influence the surface tension and viscosity will decrease the size of the air bubble released from a diffuser and reduce the transfer of oxygen into the solution. The maximum reduction in oxygen transfer occurs in the region of maximum surface tension change. The effect of the addition of several organic substances on the oxygen transfer characteristics are shown.

Aeration involves the transfer of oxygen from air to a turbulent liquid. In diffused aeration air bubbles are formed at an orifice from which they break off and rise through the liquid, finally bursting at the liquid surface. The transfer process is considered to occur in three phases: during bubble formation, during bubble rise through the liquid depth, and as the bubble bursts at the liquid surface. Oxygen transfer during the initial and final phases of the bubble's life may be considered as end effects which will be substantially constant for a given aeration system.

In diffused aeration oxygen transfer during the bubble rise can be related to the characteristics of the bubbles released from a submerged orifice. The bubble characteristics can usually be defined in terms of a Reynolds number (*1*). At Reynolds numbers less than 300 to 400 the bubbles are spherical and act as rigid spheres. This corresponds to an approximate bubble diameter of 0.2 cm. Over a Reynolds number range of 400 to 4,000 the bubbles assume an ellipsoidal shape. In this range McKeown and Okun (*2*) have shown that the bubble formed has an inverted pear shape. In the early stages of the bubble's life, as it rises through the liquid, the bubbles are not in equilibrium with the surrounding liquid, and they oscillate between a fluid sphere and an elongated ellipsoid in decreasing amplitude. At Reynolds numbers greater than 4,000 the bubbles form spherical caps.

In the range of Reynolds numbers less than approximately 1,000 the liquid film coefficient in pure water has been related to the physical characteristics of the aeration system through an empirical correlation of the Reynolds and Sherwood numbers (*3.*) The end effects, which result in a decreasing transfer coefficent with increasing liquid depth, are included in the correlation as an exponential function of depth:

$$\frac{K_L D_B}{D_T} \cdot h^{1/3} = c\,\frac{D_B v_B \rho}{\mu} \qquad (1)$$

It was found that this empirical depth correction holds well for liquid depths in excess of 100 cm. Results obtained by several investigators and by the authors are shown in Figure 1. The effect of depth can also be estimated by plotting N_{Re}/N_{Sh} vs. liquid submergence depth. The average results and the spread of the data over a wide range of air flows and bubble diameters are shown in Figure 2. It is interpreted from this plot that extension of the curve to the ordinate (zero depth) estimates the end effects. Evaluation of the individual set of data employed in Figure 2 has shown that the slope and intercept of this form of plot vary somewhat with the bubble characteristics and the diffusion device. Further study is in progress to more theoretically define end effects during bubble aeration.

For the range of submergence depths normally encountered in aeration practice Equation (1) can be rearranged to define K_L for a specified operating condition:

$$K_L = c_1 \frac{v_B}{h^{1/3}} \qquad (2)$$